Zhong *et al. Int J Concr Struct Mater* (2021) 15:28
https://doi.org/10.1186/s40069-021-00461-0

International Journal of Concrete Structures and Materials

RESEARCH Open Access

Flexural Capacity Prediction Model For Steel Fibre-Reinforced Concrete Beams

Aocheng Zhong, Massoud Sofi*, Elisa Lumantarna, Zhiyuan Zhou and Priyan Mendis

Abstract

Steel fibre (SF) reinforcement has been shown to improve the ductility of high strength concrete (HSC), which is known to be brittle. Research conducted to date on steel fibre reinforced concrete and its effects have emphasised post-failure performance and cracking mechanism. The difficulty in predicting the behaviour of fibres is due to the randomly distributed nature of the material within the matrix leading to a probability distribution of results. Published literature has shown a benefit of adding steel fibres in terms of the ductility performance of structures. Clearly, there is a potential for such material as replacement of conventional steel reinforcement. This study proposes a theoretical model of evaluating the potential of using steel fibres as a replacement material to conventional steel reinforcement bars based on the case study, laboratory and theoretical methodologies. The compressive strength of the concrete at key dates, the effective fibre cross-sectional were measured, and a prediction model was created based on the measurement parameters. The use of four-point flexural testing, standard compressive testing and software image modelling provided the study with relevant data used to analyse and compare to the prediction. Greater ductility performance and toughness were observed with increased fibre volumes, confirming proposed predictions and conclusion drawn from published literature. No consistent or conclusive correlations between fibre volumes and the compressive strength of concrete were found. A relationship between fibre volumes and predicted moment capacities of steel fibre reinforced concrete beams was found based on the proposed theoretical flexural analysis method.

Keywords: Steel fibre, Moment capacity, Flexure, Early age concrete

1 Introduction

High Strength Concrete (HSC) use in modern construction is becoming increasingly popular as opposed to Normal Strength Concrete (NSC). HSC has inherent favourable properties such as higher mechanical properties, a more linear behaviour under load and reduced micro-cracking when subjected to higher loads. These enhanced material properties allow for the design and construction of smaller member sections compared to NSC when expected to undergo the same load levels. HSC offers a more cost-effective solution (Diniz & Frangopol, 1997; Wu, 2010).

One of the drawbacks of the application of HSC is its inferior ductility performance when compared to NSC. From a structural safety point of view, the design for ductility is as important as strength properties (Ho et al., 2004). Ductile performance gains even more importance when considering the seismic design of structural members. It is a key determinant of structures' ability to deform inelastically without encountering fracture or brittle structural failure.

Many studies have been conducted to design and improve the ductility performance of HSC structures (Chunxiang & Patnaik, 1999; Mydin, 2013; Tablan, 2007). Many failures have been observed during construction because of intrinsic thermal and/or mechanical stresses imposed on maturing concrete (Sofi et al. 2014, 2019). In summary, it is established that if the correct design approach is adopted, the ductility of HSC can be restored

*Correspondence: massoud@unimelb.edu.au
Department of Infrastructure Engineering, The University of Melbourne, Melbourne VIC 3052, Australia
Journal information: ISSN 1976-0485 / eISSN 2234-1315

to the levels of NSC (Pam et al., 2001). Addition of steel fibres has been shown to improve ductility properties. For instance, Tablan (2007) has explored the inclusion of various types of fibres within the HSC mix to improves its ductile performance. These include naturally occurring coconut fibres and steel fibres (Tablan, 2007).

Steel Fibre (SF) reinforcement is the most widely used material in structural concrete. The popularity of SF is due to its low water absorption characteristics, increase in impact and abrasion resistance properties, its lower maintenance and increased durability compared to other types of fibres. Other factors include economy and savings will be greater for heavier crack control systems. Studies found that the inclusion of SF at approximately 0.75%–1.00% content in volume within a concrete mixture helped improve its ductility tensile and flexural strength properties (Mydin, 2013). Similarly, Chunxiang and Patnaik investigated the effects of SF on HSC beams with longitudinal reinforcement.

Results showed that fibre reinforcement led to an increased flexural rigidity before yielding and improved ductility performance due to an increased displacement at failure (Chunxiang & Patnaik, 1999). Further research into SF and its impact on strength, such as compressive and flexural capacity, have been undertaken. In addition to improving ductility performance, the presence of SFs improve the tensile and flexural capacities of HSC (Song & Hwang, 2004).

A study by Hsu and Hsu analysing multiple cylindrical specimens, both with and without confinement, presented a stress–strain relationship of Steel Fiber Reinforced Concrete (SFRC). Results suggested that there was a clear increase in post-peak loading stresses at any given strain level, hence improving the ductility and toughness (Hsu & Hsu, 1994).

There is currently no predictive models describing the effect of the addition of SF accurately due to the irregular distribution and orientation of fibres across the member section.

Current methods described in AS 5100.5–2017 used to determine the strength capacity of proposed steel fibre reinforced concrete (SFRC) structural elements relies solely on the individual testing of each composite mixture (Standards Australia, 2017). The test is required before the use of SFRC, thus limiting its potential application and inclusion in early design phases of construction projects.

1.1 Fibre Bond Stress-Slip Relationship

Influences on both the average interfacial bond stress and the pullout load per fibre were investigated as early as 1984 (Mangat et al., 1984). The effect of several parameters, such as spacing and aspect ratio, fibre embedment length, and diameter on the interfacial bond strength between the steel fibres and mortar matrix was experimentally investigated. A flexural load was generally applied to simulate the state of stress commonly experienced by the structural elements. The investigation established that the average pullout bond strength per fibre increases with increasing fibre embedment length and decreases with increasing fibre diameter. Further, the authors have found that fibres spacing has no significant influence on bond strength. The average bond stress decreases when the cement matrix is modified with steel fibre reinforcement, the reduction being greater at higher fibre contents. The effects of matrix strength, hooked-end fibre embedment length and orientation were later investigated (Robins et al., 2002). It was found from the studies that the pullout response of a hooked-end fibre is mainly influenced by three parameters: fibre embedment length, fibre orientation and matrix strength. The pullout response was characterised by one of two pullout modes: either the hooked-end is straightened as it is pulled out from the matrix or the fibre fractures at the hook portion. The matrix strength increases the magnitude and toughness of the pullout response. As the fibre orientation deviates from the direction of the pullout load, its response becomes increasingly less influenced by matrix strength and increasingly on the mechanical properties of the fibre itself as it attempts to straighten in line with the direction of load.

1.2 Numerical Models To Predict The Performance Of SFRC

To lower the hurdle of considering SF in the early design phase, various theoretical models have been proposed to find the effects of SF on the concrete properties. A model derived to estimate the upper and lower bounds of the tensile strength of SFRC (Grimaldi & Luciano, 2000), was shown to accurately model the tensile strength of SFRC. However, drawback from this model is the complexity of analysis and theoretical application which make it difficult for useful day-to-day application (Olivito & Zuccarello, 2010). Alternatively, a regression analysis conducted on varying SFRC mixtures demonstrated that there is a simple yet direct relationship between volumetric fibre content and flexural and tensile strengths (Song & Hwang, 2004).

A correlation between SF content and tensile strength is seen to be evident, therefore, providing justification for expanding research into analysing the effect of SF on ultimate flexural strength capacities. Studies investigating SF discussed above rely heavily on a theoretical approach, with limited laboratory testing or other methods. The conclusion drawn from models seems to be valid. However, the complexity of mathematical modelling and

forecasting provide limitations of these models in day-to-day application.

A theoretical model based on fibre surface abrasion was developed for synthetic fibres to predict the load–displacement relationship (Wang et al., 1988). The effects of Poisson's ratio, elastic-frictional bond strengths, and bond strength variation with slippage distance on the pullout relation were investigated. Bond strength was found to increase with the slippage distance during the process of pullout. Hajsadeghi et al., (2018) used contact elements to simulate the fibre-matrix interaction in which the Coulomb friction model was used to account for the physicochemical bond and the fibre-matrix interface friction. The model considered geometric and material nonlineariti3es accurately simulating the steel fibre pullout mechanism and showing good agreement with the experimental results. They suggested that their proposed model could be used to conduct parametric studies with the aim of designing and optimisation of new types of steel fibres. They noted that cracks could initiate at any point along the fibre which typically slips on the shorter embedded side. This will affect the pullout performance of steel fibres, especially those which are fully deformed such as crimped and twisted. They suggested that a pullout study should be performed on fibres with various embedded lengths and angles of inclinations.

1.3 SF Measurement And Effective Area

There is a degree of uncertainty when it comes to the distribution of fibres, as they are orientated and located randomly throughout a concrete sample. This makes their contribution within a sample and their proportion as tensile reinforcement very difficult to measure. Soroushian and Lee (1990) attempted to analyse SF distribution within cross-sections of concrete beams. It was concluded that the distribution of SFs is influenced directly by both the boundaries conditions, the beam cross-sectional area and the vibration placement of SFRC (Soroushian & Lee, 1990). The vibrational placement was shown to settle down and reorient fibres horizontally. To calculate flexural capacities of SFRC, a relationship between volumetric fibre content and the effective area of cross section of the SFRC was proposed. To evaluate the effective area, a method of dividing the cross-section of the SFRC beam into three regions (top, middle and bottom) was proposed. Each region has then been given an orientation factor, which could be modelled into an effective area of that region. All three effective areas were then implemented in a theoretical relationship, resulting in an overall effective area for the cross-section. Results found that the effective area of SF within a cross-section is only 54% effective compared to the effective area with SF with the most desirable alignment. This is due to the random orientation of fibres throughout the section (Soroushian & Lee, 1990).

Another method used to determine SF cross-sectional area is the destructive methods of cutting and polishing concrete specimens. From the cross-section obtained, the area of fibre in a cross-section can be determined through software imaging analysis. Destructive measurement of SF area is found to be the most accurate method to determine SF cross-sectional area (Akkaya et al., 2000).

1.4 Research Significance

Through the combination of a proposed theoretical model based on classical flexural stress distribution model and laboratory data obtained around SF, the study aims to draw some simple yet meaningful relationships between SF and its subsequent interaction with concrete. The interaction between SF and key structural properties of concrete such as ductility and flexural behaviour will be investigated. As a result, the outcomes of the study will contribute to expand the database on SFRC and lead to further research in the field.

2 Proposed Flexure Analysis Model of SFRC

The classic flexure strength utilises the principle of force equilibrium and the mechanical properties of concrete and steel. It assumes a uniform compressive stress distribution in the concrete section above the neutral axis and tensile stress in the reinforcement bars below the neutral axis. The ultimate moment capacity is then determined through the coupling between the tensile and compressive forces. The expression is indicated in Eq. 1:

$$M_u = A_{st} f_{sy} d \left(1 - \frac{A_{st} f_{sy}}{1.7 b d f_c^{'}}\right) \quad (1)$$

where M_u is the ultimate flexure strength of the RC subject to bending, A_{st} is the cross-sectional area of steel reinforcement, f_{sy} is the yield strength of steel, $f_c^{'}$ is the characteristic strength of concrete and b and d are the width and effective depth of the cross section of the concrete member, respectively.

The same principle applies to an SFRC in a sense that the element resists bending through compression on concrete and tension on the fibres. Yet, due to the mixing technique currently employed, it would be difficult to determine the location and orientation of each fibre along a cross-section. However, if a random distribution is assumed, there exists a possibility to simulate the effect of randomly scattered fibres using an equivalent reinforcement bar with an effective area and position, as presented in Fig. 1. Therefore, the problem can be reduced into two main categories: the determination

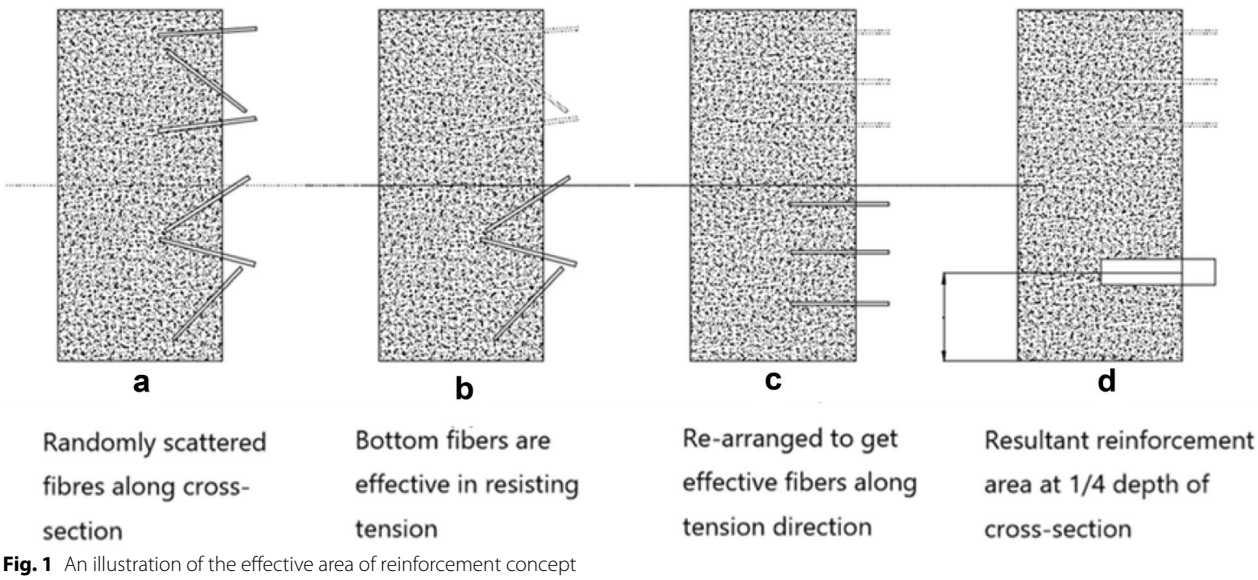

Fig. 1 An illustration of the effective area of reinforcement concept

of effective area and the prediction of the resultant location of the equivalent reinforcement bar.

Assuming the random nature of the steel fibre location, with enough data points, the fibres can be divided into two equal groups of reinforcement bars at 1/4 and 3/4 of the depth. The top fibres can be assumed to have a negligible effect on the ultimate moment capacity. This implies that only half of the fibres are effective in resisting bending moment. Therefore, if all fibres are aligned in the longitudinal direction, the effective area that resists bending would be:

$$A'_t = 0.5A'_g \tag{2}$$

where, A'_t is the gross area of SF that will be in tension and resisting bending, A'_g is the gross cross section area of the SF. The resultant position of the fibres is at 3/4 depth of the section measured from the top extreme fibre (or 1/4 from the bottom), as indicated in Fig. 1.

However, as the orientation of the fibres is not always pointing to the desired direction (i.e. perpendicular to the direction of the cracks), it is necessary to account for the effect of random distribution of the fibres' orientations. Consider Fig. 2 which shows the orientation of a single steel fibre along a cross section, θ_i is the angle of rotation of the fibre with respect to the horizontal axis (perpendicular to the cross-section). The angle has a value between 0 and 90°, A_i is the cross-sectional area of one individual fibre. The cross-sectional area of the fibre along the cutting surface (the cross section of the member), A'_i would be:

$$A'_i = \pi r^2 sec(\theta_i) = A_i sec(\theta_i) \tag{3}$$

Assuming there are n numbers of fibres crossing the same cutting surface in the tension region, the overall area of the fibre reinforcement is:

$$A'_t = \sum_{i=1}^{n} sec(\theta_i)\pi r^2 = nA_i \sum_{i=1}^{n} sec(\theta_i) \tag{4}$$

Furthermore, as the fibres would only be effective in the longitudinal direction in resisting tension, Eqs. 5 and 6 can be expressed (considering Fig. 2 again) as:

$$A'_{i.eff} = \pi r^2 cos(\theta_i) = A_i cos(\theta_i) \tag{5}$$

$$A'_{eff}. = \sum_{i=1}^{n} cos(\theta_i)\pi r^2 = nA_i \sum_{i=1}^{n} cos(\theta_i) \tag{6}$$

where, A'_{ieff} is the area of SF resisting tension considering the orientations of the fibres. Combining Eqs. 4 and 6 yields the following relationship:

$$k = \frac{A'_t}{A'_{eff}} = \frac{\frac{\sum_{i=1}^{n} sec(\theta_i)}{n}}{\frac{\sum_{i=1}^{n} cos(\theta_i)}{n}} \tag{7}$$

where, k is the effective steel fibre area factor, i.e., the ratio between A'_t and A'_{eff}. A'_t can be determined using an appropriate approach such as photogrammetry analysis of the cross sections which equals to half of the overall SF area of a cross section A'_g of a concrete member.

While the exact value of the term $\frac{\sum_{i=1}^{n} sec(\theta_i)}{n}$ and $\frac{\sum_{i=1}^{n} cos(\theta_i)}{n}$ depends on the magnitudes of corresponding

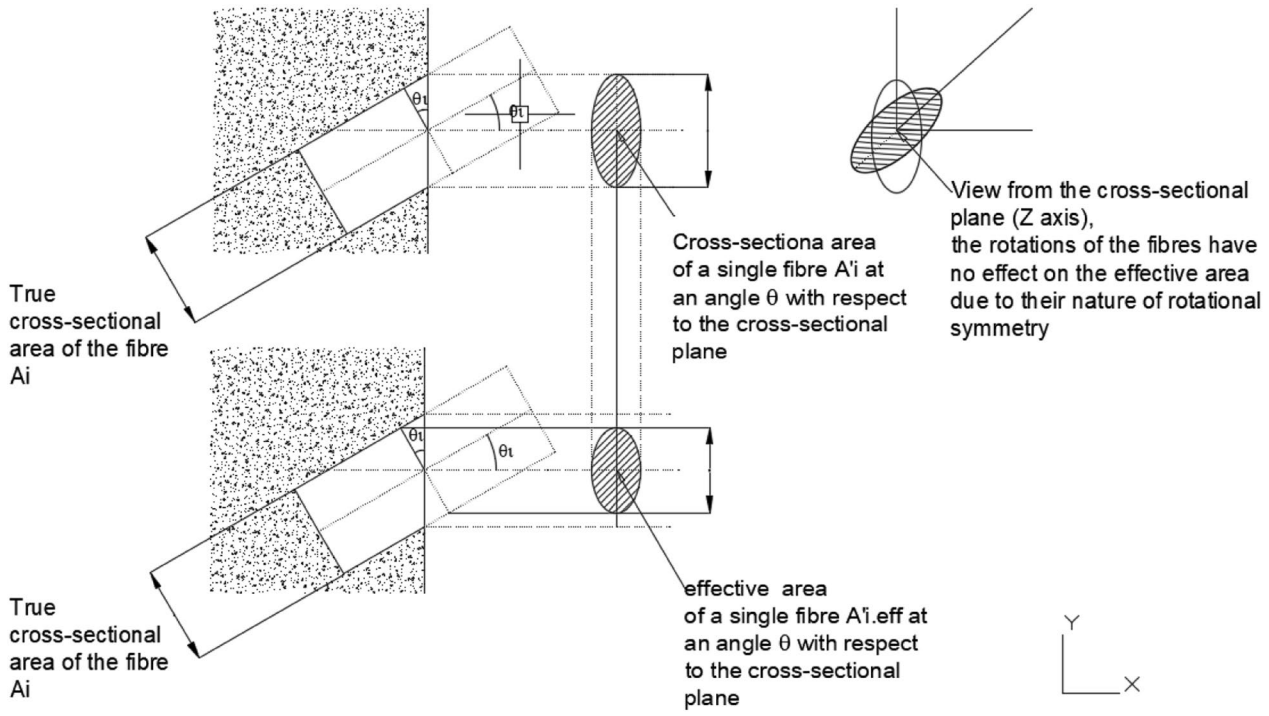

Fig. 2 Effective area and cross-sectional area of a single fibre- a close up

notations in the expressions, at a large number of n, the "law of large numbers (LLN)" governs. The LLN indicates the average of the results obtained from many trials should approach the expected value and will become even closer with more trials. The orientation of the fibres could be considered independent from each other. Hence, the number of fibres is equivalent to the number of trials. Therefore, finding the value of $\frac{\sum_{i=1}^{n} sec(\theta_i)}{n}$ is effectively a question of finding the expected value of $sec(\theta_i)$ for $0 < \theta_i < 90°$, as $sec(90°) = +\infty$. Limiting θ_i to be no greater than $tan^{-1}(l_{SF}/2r)$ should effectively avoid non-divergence, where l_{SF} is the length of the steel fibre and r is the fibre radius. Solving the mean of $\frac{\sum_{i=1}^{n} sec(\theta_i)}{n}$ and $\frac{\sum_{i=1}^{n} cos(\theta_i)}{n}$ using standard integration method (Eqs. 8 and 9) should yield the expected ratio between the overall fibre area along a cross section to the effective area of fibre resisting tension.

$$\bar{cos}\ (\theta) = cos\left(\frac{\int_a^b \theta.cos(\theta)}{\int_a^b cos(\theta)} d\theta\right) \tag{8}$$

$$\bar{t}\ sec(\theta) = sec\left(\frac{\int_a^b \theta.sec(\theta)}{\int_a^b sec(\theta)} d\theta\right) \tag{9}$$

where $\bar{cos}\ (\theta)$ and $\bar{sec}\ (\theta)$ are the expected value of $\frac{\sum_{i=1}^{n} cos(\theta_i)}{n}$ and $\frac{\sum_{i=1}^{n} sec(\theta_i)}{n}$ respectively, a and b are boundary values of the angle of rotation, in this case $0 < \theta_i < \tan^{-1}(\frac{l_{SF}}{2r})$.

With the effective area of fibre established and the resultant position determined, the classical flexural strength equation can be modified and written as:

$$M_u = A'_{eff} f_{sy} d\left(1 - \frac{A'_{eff} f_{sy}}{1.7bdf'_c}\right) \tag{10}$$

Equations 7, 8, 9 and 10 describes the simplified numerical model proposed for the flexural analysis of SFRC under pure bending.

3 Experiment

A series of laboratory tests were performed in the study to acquire the necessary inputs to validate the proposed model. A typical Grade 32 slab mix with 35% replacement of fly ash was adopted in the study incorporating three concentration rate of steel fibre (0%, 0.75% and 1.5% volumetric content).

3.1 Concrete Mix Details

The composition of concrete is shown in Table 1.

The three steps in preparing the test specimens included mixing, cast and curing of the samples. The preparation of concrete mixes in the laboratory follows AS1012.4 (Standard Australia, 2014). Coarse aggregates

Table 1 Concrete mix composition

Material	Cement	Fly ash	Water	Fine aggregate	Coarse aggregate	Admixture
Quantity (kg/m^3)	293.08	157.81	165.52	581.41	1000.85	1.15

were placed in a mixer and mixed for 3 min. Then binder materials were added and mixed for another 3 min. Thereafter, the liquid phase was added, and the mixing continued for an extra 4 min.

3.1.1 Specimen Preparation And Curing

The mechanical properties of the concrete mix were determined according to standard test procedures. Specimens were prepared in accordance with AS 1012.8.1 (2014). Specimens used for compressive strength testing were cast in cylindrical moulds with height and diameter dimensions of 200 mm × 100 mm, respectively.

Specimens used for four-point bending testing and cross-sectional analysis were cast using rectangular beam moulds with an internal dimension of 100 mm × 100 mm × 400 mm. They were cast for 4-point bending test following ASTM E72-15 (2015) to capture the ultimate flexural strength. All test specimens were compacted using a vibration table to remove air bubbles. For each type of mixture undergoing different curing duration, three samples were prepared for both compressive and flexural strength test.

Finally, all test specimens were stored under laboratory conditions 23 °C ± 2 temperature for curing until the time when they were prepared for testing.

3.1.2 Steel Fibre Properties

A commercial SF DRAMIX® 4D product was used in the study. The total length (l_{SF}) of the steel fibre is 60 mm with a diameter (d) of 0.9 mm and aspect ratio of 65. Tensile strength of individual fibres is 1500 MPa (tolerance ± 7.5) and Young's Modulus of 210,000 MPa. The fibres conform to ASTM A820 (2006) and BS EN 14,889–1:2006 (2006). The fibres come as networks which include 3200 fibres/kg. They were treated according to the DRAMIX® 4D recommendations for handling, dosing and mixing.

3.1.3 Experiment Procedures

The experimental programme consists of four major testing methods for data acquisition. They were the standard compressive test, modulus of elasticity test, four-point bending test and cross-sectional SF area analysis. Except for the cross-sectional SF analysis, all testing procedures were used to test specimens at age 1, 3, 7 and 28 days. A summary of the details of the tests are provided in Table 2.

As highlighted previously in Sect. 1.2, the measurement and approximation of SF cross-sectional area is a complex task and one that has not been fully developed theoretically. For this study, two beam samples (one with 1.50% SF volume and the other with 0.75% SF volume) were cut at different cross sections using a circular drop saw. In total, six cross sections were obtained from each beam. These sections were then digitalised with a high resolution (42-mega pixel Sony A7Rii) camera, allowing for computer analysis to obtain SF area approximations. The software used to analyse cross-sectional images was "Image-Pro Plus" that can recognise and calculate the area of the SF at each cross-section.

4 Results and Analysis

4.1 Mechanical Properties of SFRC Specimens

Table 3 below summarises the tested ultimate compressive strengths, and the respective maximum axial loading experienced.

Figure 3 shows the comparison of compressive strength between fibre content samples as curing age increases. The maximum loading recorded during the 4 point bending test is summarised in Table 4. The maximum load is

Table 2 Details of testing procedures

	Compressive test	Four-point bending test	Cross-sectional SF area analysis
Standards	AS1012.9:2004	ASTM E72 – 15	N/A
Apparatus Used	Tecnotest KE300/CE	Nstron 5569A and MTS Exceed E45	Diamond Cutter/ High resolution Digital Camera
Loading Rate	N/A	0.5 mm/min (0% SF) and 0.75 mm/min (with SF)	N/A
Sample Tested	Cylinder	Beam	Beam
No. Sample Tested	24	12	2
Data obtained	Compressive strength	Flexural Strength and force–displacement Curve	6 cross sections SF distribution profile on cross sections

Table 3 Compressive testing results

Steel fibre	Mean compressive strength (MPa)		
Volume (%)	0.00%	0.75%	1.50%
1 day	15.45	17.00	12.21
3 days	22.65	26.75	21.02
7 days	25.78	28.20	31.05
28 days	34.15	28.98	32.39

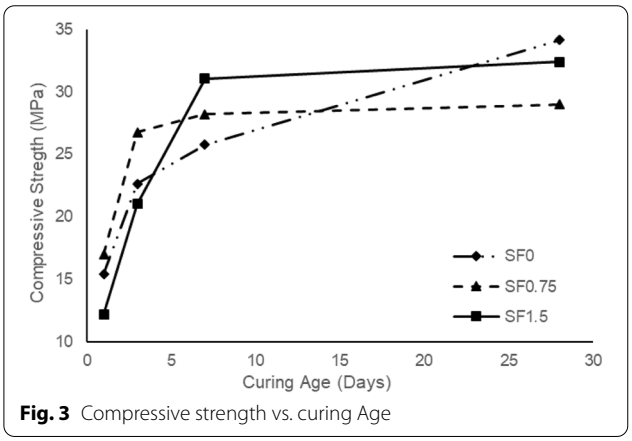

Fig. 3 Compressive strength vs. curing Age

Table 4 Four-point flexural testing results

Steel fibre	Maximum applied load (kN)		
Volume (%)	0.00%	0.75%	1.50%
1 day	16.82	33.86	35.97
3 days	21.88	33.73	41.10
7 days	24.60	43.57	52.50
28 days	27.20	49.95	65.24

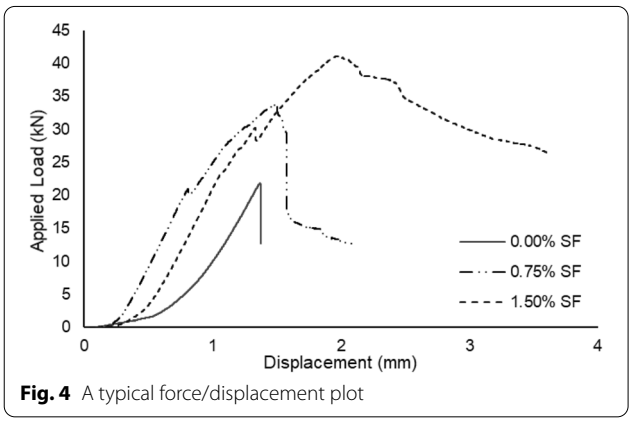

Fig. 4 A typical force/displacement plot

Table 5 Measured moment capacity

Steel fibre	Ultimate moment capacity (kNm)		
Volume (%)	0.00%	0.75%	1.50%
1 day	0.53	1.06	1.12
3 days*	0.68	1.05	1.28
7 days	0.77	1.36	1.64
28 days	0.85	1.56	2.04

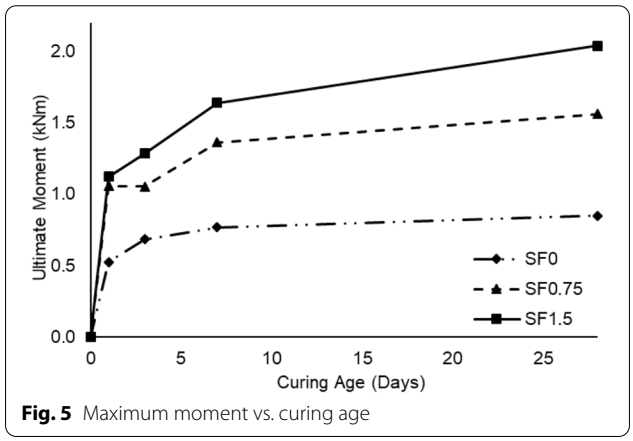

Fig. 5 Maximum moment vs. curing age

plotted against the displacement at mid span in Fig. 4. Table 5 summarises the calculated flexural capacities based of the maximum applied loading for each sample. Figure 5 presents the comparison of flexural capacities between fibre content samples as curing age increases.

Figure 3 shows that there is no clear trend on the effect of steel fibres on the compressive strength of concrete. As curing age increases, the compressive strength of the specimens with each fibre content specimen (control mix, 0.75%, and 1.50%) do not deviate significantly from the control specimen (without SF content). The findings confirm previous research which found negligible improvements in the compressive strength of concrete due to the addition of steel fibres (Hsu & Hsu, 1994).

Figure 4 and Table 5 indicate that both the flexural and post-peak performance increase with the increasing content of steel fibres. These observations were also reported in the literature (Song, 2004; Soroushian, 1990). This finding further validates the use of steel fibres as an appropriate method of reinforcement for concrete to increase its ductility. This is essential for high strength concrete as ductility is normally a major concern.

4.2 Cross-Sectional Area of Steel

The process of determining the cross-sectional area involves treating each of the cross-sectional image to identify the SFs and determine the cross-sectional area

Table 6 SF Area determined through photogrammetry analysis (mm^2)

	Steel fibre volume	
Cross sections (mm^2)	**0.75%**	**1.50%**
1	188.80	316.20
2	211.51	345.50
3	184.05	275.60
4	152.16	326.47
5	175.78	399.60
6	192.18	255.58
Mean	184.08	323.16
Standard deviation	19.63	51.31
Coefficient of variance	0.11	0.16

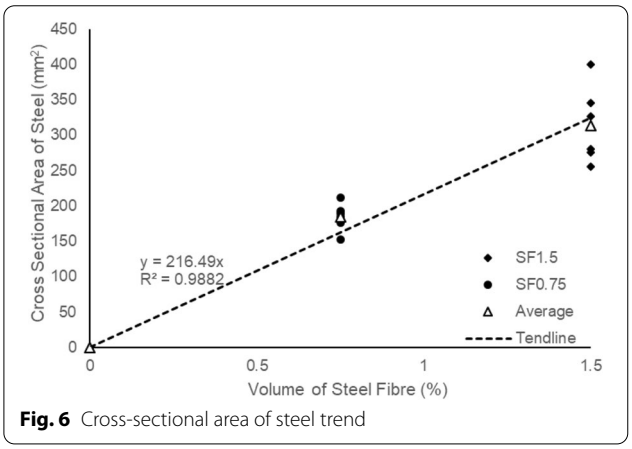

Fig. 6 Cross-sectional area of steel trend

of each fibre, which was then added to obtain the total cross-sectional area of the steel.

Table 6 summarises the area of steel measured using the image processing software for each of the twelve cross-sections obtained from beams, six of which have 0.75% and six that have 1.50% fibre content. The standard deviation of the cross-sectional area of steels associated with 1.50% of fibre content is higher compared to 0.75% fibre content, which is to be expected.

An average was then calculated as a mean of establishing a trend of the cross-sectional area of steel against volumetric fibre content. The observed trend is shown in Fig. 6, following a presentation of the taken and treated image of a typical cross-section in Fig. 7.

4.3 Effective Area of Steel and Flexural Analysis

The expected ultimate flexural strength of the SFRC specimens can be estimated based on the proposed equations presented in Sect. 2. The limiting angle is calculated to be 89.1° based on the dimensions of the fibre. The ratio between $A^{'}$ and $A^{'}_{i.eff}$ can then calculated by solving Eqs. 8 and 9 using the integration method. The value of the ratio was calculated to be 3.10. Solving Eq. 10 utilising the input of gross SF area from Table 7 and specimen dimensions from Sect. 3.1.1 gives the estimated ultimate moment capacity as indicated in Table 8, comparisons of the measured and predicted ultimate moment capacities are presented in Figs. 8 and 9.

The reason for the M_u predicted to be relatively insensitive to the curing age is due to a very small dosage of steel fibres which results in a very small effective reinforcement area. This leads to the fractional term $\frac{A_{st}f_{sy}}{1.7bdf^{'}_{c}}$ in Eq. 1 relatively small, and therefore the change in the compressive strength of concrete does not appear to affect the predicted values (Fig. 9). For instance, if one takes 0.75% SFRC case as an example, in the 100 mm × 150 mm beam specimen, the effective reinforcement area is only 29.7 mm^2. This will result in the fractional term value of only 0.0343. However, if the dosage of SFRC is increased to the extent that the effective reinforcement area is equivalent to the area of the rebars, at a balanced flexural design condition (i.e., reinforcement to cross-sectional area ratio = 0.0324), the reinforcement area should be at 486 mm^2 for the same beam specimen. Assuming this value, M_u predicted will observe significant variation as a result of the change in $f^{'}_{c}$ as shown in Table 9.

However, testing samples cast at this steel fibre dosage (i.e., at 486mm^2, SF dosage of 12.6%) would result in beams with a flexural strength beyond the testing instrument's capacity. This constitutes the limitation of the study. The authors are considering a series of full-sized samples to provide further validation to the proposed model. The results reported herein should be considered interim and not directly used for the design of flexural members.

4.4 Effective Area of Steel in Tension

As can be observed in Fig. 6 and Table 6, the average of the total measured area of steel for 0.75% and 1.50% SFRC is 184 mm^2 and 319.83 mm^2, respectively. The standard deviation and the coefficient of variation imply that the variation in the area of steel increases as the fibre content increases. Given the random nature of steel fibre orientation and position, this is expected. It is worth noting that the ratio between the total area of steel with 1.5% SFRC to its counterpart with 0.75% SFRC is 1.76. At perfectly random distribution, this ratio, however, should be at 2. The difference could be contributed by the law of probability, which dictates that the accuracy of the average area of steel is limited by the number of cross-section samples measured and the volumetric content of fibres in

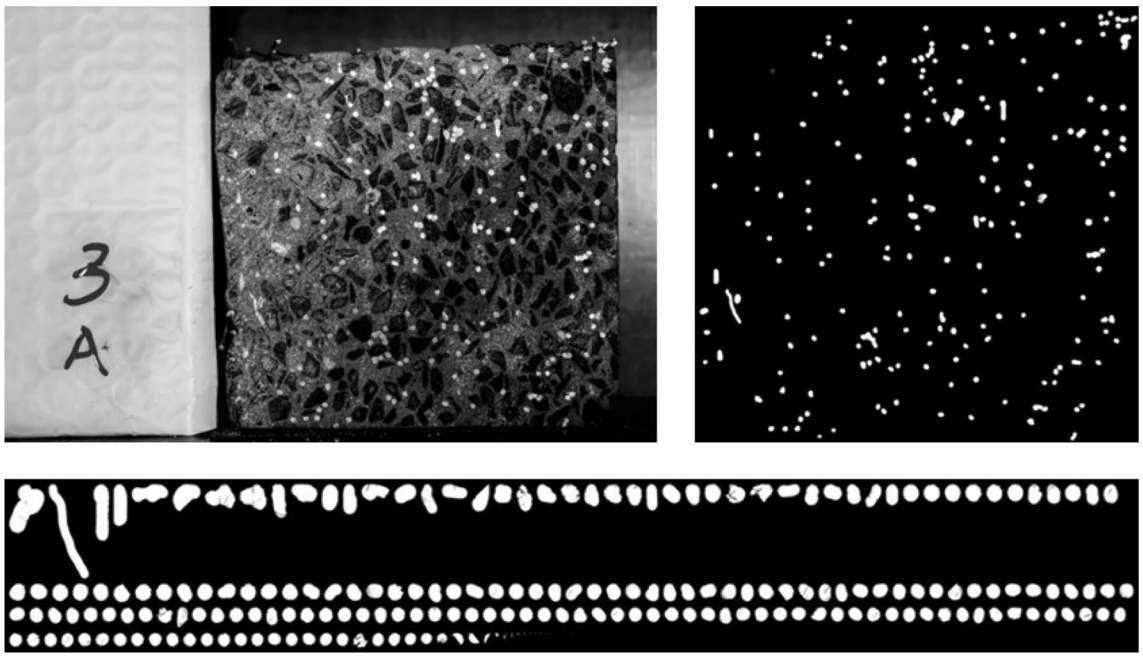

Fig. 7 A presentation of the processed SF area along a cross-section

Table 7 Determined effective area of SF in resisting tension

Steel fibre	A'_g	A'_t	A_eff'
Volume	mm^2	mm^2	mm^2
0.75%	184.08	92.04	29.74
1.50%	319.83	159.91	51.66

the specimen. Given the inherent randomness of the steel fibre location and orientation, with six samples for each fibre content, an accurate average cannot be gauged. Further, the true random behaviour of fibres can be reduced by vibrating the specimens after moulding (Soroushian & Lee, 1990) as the vibration causes the fibres to settle towards the bottom and rotate towards the horizontal. The uncertainties with determining the average area of steel from the limited number of samples and the known effect of the concrete vibration on the randomness of fibres highlight the difficulties in estimating the reinforcement area of SF in any given cross-sections. More samples are required to produce a more accurate and reliable trend line. However, as the authors used the actual measured value of SF reinforcement area in their predictive model, the inaccuracy was found to be inconsequential to the findings and a standard flexural analysis can be used to reliably predict the moment capacity of SFRC. This is discussed further in Sect. 4.5.

4.5 Prediction of Ultimate Moment Capacity

This paper highlights the potential use of the classical flexural strength analysis method, in conjunction with an effective steel fibre area factor (k) determined through statistical analysis. The method has the potential to reduce the complexity in the current theoretical predictions of SFRC and determine flexural capacities of SFRC without the need for experimental testing.

Table 8 Calculated ultimate moment capacity

Steel fibre	0.75%				1.50%			
Curing age (days)	1	3	7	28	1	3	7	28
f'_c (MPa)	17	26.7	28.2	28.9	12.2	21.0	31.0	32.4
Mu Predicted (kNm)	1.115	1.115	1.115	1.115	1.937	1.937	1.937	1.937
Mu measured (kNm)	1.058	1.054	1.362	1.561	1.124	1.284	1.641	2.039
Calculated /Measured	1.05	1.06	0.82	0.71	1.72	1.51	1.18	0.95

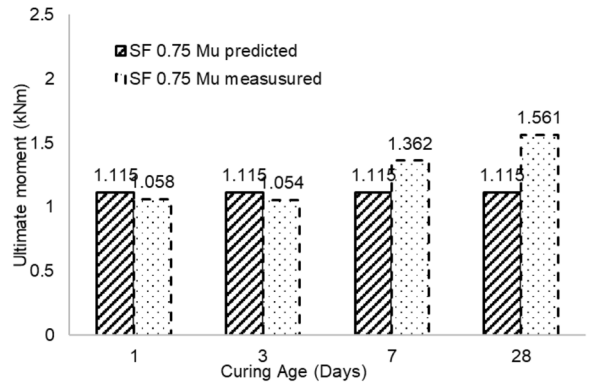

Fig. 8 Comparison between predicted and measured ultimate moment capacity at each measured date-0.75%SFRC

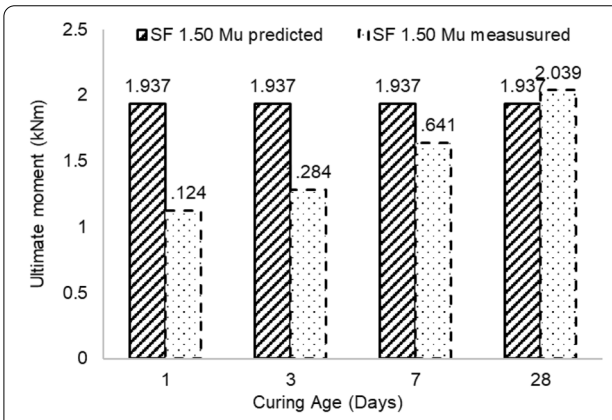

Fig. 9 Comparison between predicted and measured ultimate moment capacity at each measured date-1.50% SFRC

Table 9 Variation of M_u predicted as a function of $f_c^{'}$ for a higher dosage of SFRC

$f_c^{'}$(MPa)	17.0	26.7	28.2	29.0
M_u predicted (kNm)	16.02	23.4	24.1	24.4

Based on the measured compressive strength (Table 3) and the effective area of steel resisting the tensile stress, the ultimate moment capacity was calculated (Table 8). It was found that the flexural capacity of SFRC with discrete and definable reinforcement locations can be applied when reinforcement area and location are averaged from a distribution.

It can be seen from Fig. 8 and 9 that, with the increase in compressive strength of concrete, the measured ultimate moment capacities increases while the predicted capacities only rise slightly due to the insensitivity of the prediction to changes in the compressive strength

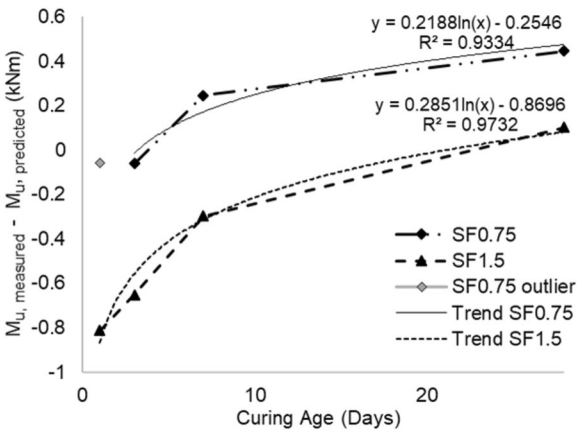

Fig. 10 The difference between the predicted and measured ultimate moment capacity vs. curing age

of concrete. During the early age of concrete, increasing compressive strength is the only defined change. The increasing trend of the measured moment capacities is associated with the bond-slip effects of the SFs. During the early ages (1–7 days), the bond between the SF and concrete paste is not fully developed, causing a weaker link at the interface of the concrete and the fibres.

Table 8 indicates that the prediction of ultimate moment capacity is the closest to the measured value for 0.75% SFRC at day 1 and furthest at day 28. Conversely, for the 1.5% SFRC, the closest estimation is on the 28th day after casting whilst at day one, the ultimate flexural capacity is over-predicted by 72.29%. Based on the above observation, it is plausible that the prediction for the 1.5% SFRC is more accurate as indicated in Sect. 2, i.e., the larger the number of "trials", the closer the sample mean is to the expected value of the population. With more fibre content, the number of trials increases; therefore, the average reinforcement area provided through the cuts in 1.5% SFRC samples should yield a better indication of the expected value. Hence more accurate result in strength prediction at 28 days' curing age can be expected, where bond-slip effect is no longer pronounced at the time.

The difference between the predicted and measured ultimate moment capacity is plotted against the concrete age to investigate the time-dependent properties of bond-slip effect, as indicated in Fig. 10. If the first point of the SF 0.75% series is ignored, the general trend of the SF 0.75% and SF 1.5% series have very similar equations and appears to be almost parallel to each other, indicating the bond-slip effect is homogenous in the two cases. Furthermore, the trends observed are shown to be in close resemblance to the strength gain of concrete over time, implying that the

bond-slip effect has a close relationship to the maturity of concrete, which is a sensible deduction considering its mechanism.

It should be noted that the flexural capacity of SF concrete (as presented in this paper) is a relatively small step towards the adoption of a comprehensive model accounting for the presence of fibres and their resultant position in the matrix. A confident translation of this model considering the maturity of concrete, which will affect bond properties of fibre in the matrix will require considerable additional data. This will constitute the logical extension of the proposed approach and is assumed a limitation to the current model.

5 Conclusion

This study proposes a simplified prediction method to estimate the effect of SF on the flexural strength of concrete beams. The method is based on a combination of the classical stress distribution model and probability distribution. The flexural strength of SFRC specimens with 0.75% and 1.50% volumetric concentrations are estimated and compared to laboratory-measured values. The result shows that, as expected, the ultimate strength increases proportionally to the volumetric content of SF.

The proposed model can provide a reliable prediction of concrete beams tested in early ages. This is especially the case of the concrete with 1.50% volumetric concentrations which is a sensible observation considering the law of statistics. With regards to early age concrete, due to a complex bond-slip interaction, the model comes short of predicting the flexural capacity. Further investigation into the differences between the measurement and predicted value of the ultimate moment capacity indicates a homogeneous and logarithmic trend of the bond-slip effect over time for the two sets of samples tested in the current study. The logarithmic shape of the bond-slip effect resembles the trend of concrete maturity.

Overall, by assuming a perfectly random distribution of steel fibres, this study has highlighted the applicability of the standard flexural analysis method together with SF factor indicating the effective cross-sectional area of steel fibres to predict the ultimate moment capacity of SFRC.

Acknowledgements
The authors would like to acknowledge participation of Mr Fawad Akhtar and team in the experimental works and report, as part of their Masters degree Capstone Project undertaken in Infrastructure Engineering Department, Melbourne University.

Authors' contributions
AZ Writing the manuscript, experimental works, statistical analysis, editing MS Writing the manuscript, experimental works, analysing data, reviewing, editing. EL review and comments. ZZ Experimental works. PM Review and comments. All authors read and approved the final manuscript.

Authors' informations
Mr. Aocheng Zhong, Ph.D. Candidate, Department of Infrastructure Engineering, The University of Melbourne, Australia. Dr. Massoud Sofi, ARC DECRA Fellow/Lecturer, Department of Infrastructure Engineering, The University of Melbourne, Australia. Dr. Elisa Lumantarna, Lecturer, Department of Infrastructure Engineering, The University of Melbourne, Australia. Ms. Zhiyuan Zhou, Ph.D. Candidate, Department of Infrastructure Engineering, The University of Melbourne, Australia. Dr. Priyan Mendis, Professor of Civil Engineering, Department of Infrastructure Engineering, The University of Melbourne, Australia.

Funding
The financial supports from the Australian Research Council's Discovery Early Career Researcher Grant (DE170100165, DE 2017 R1) and The University of Melbourne are acknowledged.

Availability of data and materials
Not applicable.

Declarations

Ethics approval and consent to participate
Not applicable.

Consent for publication
Not applicable.

Competing interests
I confirm that none of the authors have any competing interests in the manuscript.

Received: 9 January 2020 Accepted: 13 April 2021
Published online: 03 June 2021

References

Akkaya, Y., Picka, J., & Shah, S. P. (2000). Spatial distribution of aligned short fibers in cement Standards Australia. (2017). Bridge Design Part 5: Concrete (AS 5100.5–2017) Retrieved from SAI Global.

Australian Standards (2014). Methods of testing concrete - Method 9: Compressive strength tests-Concrete, mortar and grout specimens (AS 1012.9–2014), Committee BD-42, Standards Australia, Sydney, NSW, Australia.

Australian Standards (2014). Methods of testing concrete - Method 17: Determination of the static chord modulus of elasticity and Poisson's ratio of concrete specimens (Reconfirmed 2014) (AS 1012.17–1997 R2014), Committee BD-42, Standards Australia Sydney, NSW, Australia.

Australian Standards (2014). Methods of Testing Concrete – Method of Preparing Concrete Mixes in the Laboratory, AS 1012.2: 2014), Standards Australia, Sydney, NSW, Australia.

A Standards 2018 Concrete Structures, (AS 3600, 2018), Committee BD-002 Standards Australia

ASTM A820 2006 Steel Fibres: Type I cold drawn, high tensile steel wire for use as primary reinforcing in slab-on-grade Minimum dosage rate A01

ASTM E72–15, Standard Test Methods of Conducting Strength Tests of Panels for Building Construction, ASTM International, West Conshohocken, PA, 2015, www.astm.org

ASTM International. (2015). Standard Test Methods of Constructing Tests of Panals for Building Construction (ASTM E72–15) Retrieved from SAI Global.composites. Journal of materials in civil engineering, 12(3), 272–279.

Baduge, S. K., Mendis, P., Ngo, T. D., & Sofi, M. (2019). Ductility design of reinforced very-high strength concrete columns (100–150 MPa) using curvature and energy-based ductility indices. *International Journal of Concrete Structures and Materials, 13*(1), 37

Bilodeau, A., & Malhotra, V. M. (2000). High-volume fly ash system: concrete solution for sustainable development. *Materials Journal, 97*(1), 41–48

Chousidis, N., Rakanta, E., Ioannou, I., & Batis, G. (2015). Mechanical properties and durability performance of reinforced concrete containing fly ash. *Construction and Building Materials, 101*, 810–817

Chunxiang, Q., & Patnaikuni, I. (1999). Properties of high-strength steel fiber-reinforced concrete beams in bending. *Cement and Concrete Composites, 21*(1), 73–81

Diniz, S. M. C., & Frangopol, D. M. (1997). Reliability bases for high-strength concrete columns. *Journal of the Structural Engineering. American Society of Civil Engineers, 123*(10), 1375

EN 14889–1 (2006), Fibres for concrete. Steel fibres. Definitions, specifications and conformity, pp.30–50.

Grimaldi, A., & Luciano, R. (2000). Tensile stiffness and strength of fiber-reinforced concrete. *Journal of the Mechanics and Physics of Solids, 48*(9), 1987–2008

Hajsadeghi, M., Chin, C. S., & Jones, S. W. (2018). Development of a generic three-dimensional finite element fibre pullout model. *Construction and Building Materials*, *185*, 354–368.

Ho, J. C. M., Kwan, A. K. H., & Pam, H. J. (2004). Minimum flexural ductility design of high-strength concrete beams. *Magazine of Concrete Research, 56*(1), 13–22

Hsu, L. S., & Hsu, C.-T.T. (1994). Stress-strain behavior of steel-fiber high-strength concrete under compression. *ACI Structural Journal, 91*(4), 448

Kwan, A. K. H., Chau, S. L., & Au, F. T. K. (2006). Improving flexural ductility of high-strength concrete beams. *Proceedings of the Institution of Civil Engineers-Structures and Buildings, 159*(6), 339–347

Malhotra, V.M., (2002). Introduction: sustainable development and concrete technology. Concrete International, 24(7).

Mangat, P. S., Motamedi-Azari, M., & Ramat, B. S. (1984). Steel fibre-cement matrix interfacial bond characteristics under flexure. *International Journal of Cement Composites and Lightweight Concrete*, *6*(1), 29–37.

Mydin, (2013). Engineering performance of high strength concrete containing steel fibre reinforcement. Analele Universitatii "Eftimie Murgu", ISSN, pp.1453–7397.

Olivito, R. S., & Zuccarello, F. A. (2010). An experimental study on the tensile strength of steel fiber reinforced concrete. *Composites Part B: Engineering, 41*(3), 246–255

Pam, H. J., Kwan, A. K. H., & Islam, M. S. (2001). Flexural strength and ductility of reinforced normal-and high-strength concrete beams. *Proceedings of the Institution of Civil Engineers-Structures and Buildings, 146*(4), 381–389

Robins, P., Austin, S., & Jones, P. (2002). Pull-out behaviour of hooked steel fibres. *Materials and Structures*, *35*(7), 434–442.

Sofi, M., Mendis, P., Baweja, D., & Mak, S. (2014). Influence of ambient temperature on early age concrete behaviour of anchorage zones. *Construction and Building Materials, 53*, 1–12

Sofi, M., Lumantarna, E., Mendis, P., & Zhong, A. (2019). Thermal Stresses of Concrete at Early Ages. *Journal of Materials in Civil Engineering, 31*(6), 04019056

Song, P. S., & Hwang, S. (2004). Mechanical properties of high-strength steel fiber-reinforced concrete. *Construction and Building Materials, 18*(9), 669–673

Soroushian, P., & Lee, C.-D. (1990). Distribution and orientation of fibers in steel fiber reinforced concrete. *ACI Materials Journal, 87*(5), 433

Standards Australia. (2017). *AS 5100 – 2017, Bridge design standard*. Standards Australia.

Tablan, W. O. (2007). Flexural strength of concrete beams containing twinned coconut fibers. Liceo Journal of Higher Education Research(1), 185.

Topçu, İB., & Canbaz, M. (2007). Effect of different fibers on the mechanical properties of concrete containing fly ash. *Construction and Building Materials, 21*, 1486–1491. https://doi.org/10.1016/j.conbuildmat.2006.06.026

Wang, Y., Li, V. C., & Backer, S. (1988). Modelling of fibre pull-out from a cement matrix. *International Journal of Cement Composites and Lightweight Concrete*, *10*(3), 143–149.

Wu, D., Sofi, M. and Mendis, P., 2010. High strength concrete for sustainable construction. Proceedings of the International Conference on Sustainable Built Environment (ICSBE-2010), Kandy, 13–14 December 2010.

Yin, R. K. (1998). *The abridged version of case study research: Design and method*. Sage Publications Inc.

Zainal, Z., 2007. Case study as a research method. Jurnal Kemanusiaan, 5(1).

Publisher's Note